Food & Function

# Physicochemical interactions with (-)-epigallocatechin-3-gallate drives structural modification of celiac-associated immunostimulatory peptide α2-gliadin (57-89) at physiological conditions

| | |
|---|---|
| Journal: | *Food & Function* |
| Manuscript ID | FO-ART-03-2019-000553.R1 |
| Article Type: | Paper |
| Date Submitted by the Author: | 25-Apr-2019 |
| Complete List of Authors: | Van Buiten, Charlene; Pennsylvania State University, Department of Food Science<br>Yennawar, Neela; Pennsylvania State University<br>Pacheco, Carlos; Pennsylvania State University<br>Hatzakis, Emannuel ; Penn State University, Food Science and Technology<br>Elias, Ryan; Pennsylvania State University, Department of Food Science |
| | |

# Physicochemical interactions with (-)-epigallocatechin-3-gallate drive structural modification of celiac-associated immunostimulatory peptide $\alpha_2$-gliadin (57-89) at physiological conditions

Charlene B. Van Buiten [a], Neela H. Yennawar [b], Carlos N. Pacheco [c], Emmanuel Hatzakis [d], Ryan J. Elias [a*]

[a] Department of Food Science, The Pennsylvania State University, University Park, PA, USA

[b] Huck Institute of Life Sciences, The Pennsylvania State University, University Park, PA, USA

[c] Department of Chemistry, The Pennsylvania State University, University Park, PA, USA

[d] Department of Food Science and Technology, The Ohio State University, OH, USA

[*] Corresponding author at: Department of Food Science, The Pennsylvania State University, University Park, PA, USA

*Email address:* elias@psu.edu (R. J. Elias)

**Keywords**

Celiac disease, EGCG, gliadin, gluten, tea polyphenols

**Abstract**

(-)-Epigallocatechin-3-gallate (EGCG), a major phenolic constituent of tea, has been shown to have biological activity within inflammatory pathways involved with food allergies and intolerances. Proposed mechanisms for this effect include sequestration and structural

modification of immunostimulatory proteins as a result of interactions with EGCG. The present study employs biophysical techniques including dynamic light scattering, circular dichroism and nuclear magnetic resonance to elucidate the likely mechanism(s) by which EGCG interacts with $\alpha_2$-gliadin (57-89) ($\alpha_2$g), an immunodominant peptide in celiac disease pathogenesis. We demonstrate that EGCG interacts with $\alpha_2$g in a multi-phase reaction driven by non-specific binding, resulting in the formation of polydisperse EGCG/$\alpha_2$g complexes which induce changes in peptide structure. We also show that these interactions occur at a range of pH levels associated with digestion, including pH 2.0, 6.8 and 7.5. Based on previous reports of binding specificity of enzymes and antigen presenting cells in celiac disease pathogenesis, our results provide foundational support for EGCG to prevent recognition of immunostimulatory gliadin epitopes by the body and thus prevent the inflammatory and autoimmune response associated with celiac disease.

## 1 Introduction

According to the 2007 – 2010 National Health and Nutrition Examination Survey (NHANES), the average adult in the United States consumes approximately 200 mg of flavonoids per day, the majority of which are consumed in the context of green or black tea.[1] The health benefits associated with tea and its constituent flavonoids have been extensively explored, both *in vitro* and *in vivo*.[2–5] In recent years, attention has turned to the potential for flavonoids to aid in the treatment of inflammatory disorders including inflammatory bowel disease and the alleviation of symptoms associated with food allergy.[6–10] These studies have demonstrated that flavonoids can be multi-functional with respect to prevention and reversal of the disease states investigated. One flavonoid of particular interest is EGCG, the major catechin found in green tea.

47 In models of food allergy, EGCG has been shown to mediate the degranulation of mast cells
48 via inhibition of histidine decarboxylase as well as reduce the expression of key proteins
49 involved in immune cell recruitment.[11–13] As food allergies are stimulated by contact with an
50 external antigen, "epitope masking", or physically blocking recognition of immunostimulatory
51 proteins by immune cells, has also been explored as a possible mechanism by which polyphenols
52 such as EGCG might mitigate the symptoms of food allergy. This has been demonstrated most
53 notably with peanut proteins and procyanidins from cranberries and blueberries, which were
54 shown to decrease allergen binding by IgE and attenuate histamine and β-hexoaminidase
55 release.[14] In other studies, peanut proteins have been shown to undergo conformational changes
56 upon binding to EGCG,[7] suggesting that structural modification may contribute to the decreased
57 IgE recognition described by Plundrich et al. (2017). EGCG has also been shown to structurally
58 modify ovalbumin, a major allergen found in eggs, preventing uptake of the allergen by
59 monocytes and thus attenuating the allergic response.[8]
60 Celiac disease is an autoimmune enteropathy that shares characteristics with both
61 inflammatory bowel disease and food allergies. In celiac disease, gluten proteins from wheat,
62 barley and rye stimulate a host of symptoms that primarily manifest in the small intestine,
63 inducing inflammation and damage to the enterocytes.[15] Gluten proteins are rich in proline
64 residues and feature repeat motifs of polyproline II (PPII) helices and random coils, structures
65 that are important for their recognition by key receptors in pathogenesis.[16] Tissue
66 transglutaminase (TG2) is an endogenous enzyme secreted by enterocytes in response to gluten
67 proteins passing the brush border that cross-links with gluten, preferentially deamidating
68 glutamine residues one amino acid away from proline residues.[17] Human leukocyte antigen
69 (HLA)-DQ2 (DQA1*05:01, DQB1*02:01) recognizes gluten epitopes and presents them to T

70 cells, activating the adaptive immune response which leads to destruction of small intestinal
71 architecture and secretion of antibodies against gluten and TG2.[18]
72 The present work explores the use of a dietary polyphenol (EGCG) as a gliadin protein
73 binding agent which, if successful, could represent a novel therapeutic approach for alleviating
74 celiac disease symptoms by masking binding sites and epitopes capable of being recognized by
75 TG2 or HLA-DQ2. Characterization of the etiology of the celiac disease autoimmune response
76 has led to the discovery of physiologically stable, 33-amino acid fragment of $\alpha_2$-gliadin that is
77 produced upon enzymatic digestion of gluten both *in vitro* and *in vivo*. This immunodominant
78 33-mer, $\alpha_2$-gliadin (57-89) ($\alpha_2$g; LQLQPF(PQPQLPY)$_3$PQPQPF), contains six overlapping
79 epitopes (1 α-I, PFPQPQLPY; 3 α-II, PQPQLPYPQ; 2 α-III, PYPQPQLPY) that are able to be
80 deamidated by TG2 and be recognized by HLA-DQ2.[19]
81 The tendency for proline-rich proteins such as $\alpha_2$g proteins to form PPII helices allows for
82 increased accessibility of polyphenols to potential binding sites within the proteins, favoring
83 noncovalent interactions such as hydrogen bonding, van der Waals interactions and π-π
84 stacking.[20] This phenomenon has been explored with respect to proline-rich salivary proteins and
85 wine tannins, as precipitation interactions between the two are thought to drive the oral sensation
86 of astringency. Interactions between EGCG and proline-rich salivary proteins have been shown
87 to modify the structure of salivary proteins and result in precipitation of both compounds.[21]
88 Structural characterization of $\alpha_2$g has revealed that the peptide transitions between extended PPII
89 helices and type II β-turns depending on solvent conditions and temperature,[22] suggesting that
90 structural modification as a result of binding with EGCG may also be possible.
91 The objective of the present study was to explore the potential for EGCG to bind to $\alpha_2$g and
92 to determine the structural impact of this interaction on the peptide. We sought to elucidate the

93 mechanism by which these interactions occur and define physiological factors which may
94 influence the interaction. From a functional perspective, structural modification of $\alpha_2$g via
95 interaction with EGCG may provide groundwork for developing a nutraceutical approach to
96 preventing the autoimmune response associated with celiac disease by preventing recognition of
97 $\alpha_2$g by TG2 and/or HLA-DQ2. This protective mechanism could work in conjunction with those
98 previously explored by our group, including prevention of gliadin digestion and inhibition of
99 gliadin-stimulated permeability and inflammation in the small intestine.[23]
100

101 **2 Materials and Methods**

102 EGCG (> 98% purity) was purchased from Quality Phytochemicals (East Brunswick, NJ)
103 and $\alpha_2$-gliadin (57-89) (LQLQPF(PQPQLPY)$_3$PQPQPF; MW = 3911.4 kDa; 95-97% purity)
104 was synthesized by 21$^{st}$ Century Biochemicals (Marlboro, MA).
105

106 **2.1 Dynamic Light Scattering**

107 Dynamic light scattering (DLS) experiments were carried out using a Viscotek 802 DLS with
108 OmniSIZE software (Malvern Instruments, Malvern, UK). Initial samples of varying $\alpha_2$g and
109 EGCG concentrations were screened for detectable colloids and to ensure experimental
110 concentrations remained below the turbidity threshold.
111 DLS was also used to measure the hydrodynamic radii ($R_h$), molecular weight and size
112 distribution using a mean of at least ten DLS measurements of EGCG/$\alpha_2$g complexes. EGCG
113 was added to 12.8 μM $\alpha_2$g at molar ratios of 5-50 times excess EGCG in 10 mM sodium
114 phosphate buffer, pH 6.8. Samples were prepared 1 h prior to analysis, which was carried out at
115 37 °C. Samples were filtered using a 0.45 μm membrane filter (Millipore Sigma, Burlington,

116 MA) prior to loading 12 μl of it into the quartz cuvette for each DLS measurement. $R_h$ were
117 measured based on 10 separate measurements of 10 s each. Experiments characterizing pH and
118 concentration effects on $R_h$ were carried out at pH 2.0, 6.8 and 7.5 with concentrations of 0.25
119 μM $\alpha_2$g and 0.4-50 times excess EGCG in 10 mM sodium phosphate buffer.
120

121 **2.1 Isotheral Titration Calorimetry**

122 An isothermal titration calorimeter (ITC; MicroCal Auto-iTC200, Malvern Instruments,
123 Westborough, MA) was used to measure the enthalpies of mixing for $\alpha_2$g and EGCG.
124 Experiments were conducted at 37 °C in 10 mM sodium phosphate buffer, pH 6.8 with a
125 reference power of 5 μcal/s. EGCG (3.2 mM) was titrated into a cell containing 280 μL of 12.8
126 mM $\alpha_2$g as 38 injections of 1 μL each. EGCG was injected into buffer alone as a control, and the
127 results were subtracted from the EGCG/$\alpha_2$g results. Data were integrated and analyzed using
128 Origin (OriginLabs, Inc., Northampton, MA). Each injection lasted 2 s and an interval of 300 s
129 was maintained between injections. The cell was stirred at 750 rpm throughout the experiment.
130 Buffer matching was ensured with a reference run prior to running experiments.
131

132 **2.1 Nuclear Magnetic Resonance**

133 All nuclear magnetic resonance (NMR) experiments were performed on a Bruker Avance-
134 III-HD 500-MHz instrument operating at a $^1$H frequency of 500.20 MHz using a 5-mm Prodigy
135 BBO BB-$^1$H/$^{19}$F/D Z-GRD probe at temperature of 298 K. Solvent suppression was achieved
136 using the Sinc1.100 excitation sculpting sequence.[24] Data acquisition and processing for all
137 experiments were performed with Topspin 3.2 (Bruker, Billerica, MA) and MestReNova 10.0.1
138 (Mestrelab Research, Santiago de Compostela, Spain).

139 **2.3.1 Saturation Transfer Difference NMR**

140 NMR samples were prepared immediately prior to analysis by dissolving $\alpha_2$-gliadin (57-89)
141 and each ligand in 85% $H_2O$, 15% dimethylsulfoxide-$d_6$ (DMSO-$d_6$, 99.8%, deuterium; EMD
142 Millipore, Billerica, MA) to achieve a final concentration of 0.25 mM in 500 μL. DMSO-$d_6$ was
143 used to aid with solubility. Ligand mapping experiments were performed with 25 mM ligand per
144 sample, or 100-fold excess.

145 In all STD-NMR experiments, on-resonance irradiation of peptide $\alpha_2$-gliadin was performed
146 at 1.84 ppm while off-resonance irradiation was set to 40 ppm. These conditions were selected
147 based on preliminary experimentation with the peptide and each ligand alone, ensuring that the
148 on-resonance irradiation frequency would not overlap with ligand resonances, but would fully
149 saturate the peptide (Figures S1, S2). The water peak originating from wet DMSO-$d_6$ was
150 suppressed in all experiments using the excitation sculpting pulse sequence in order to preserve
151 exchangeable protons. Spectra were acquired using 100 50-ms E-Burp pulses for selective
152 saturation of the peptide with a total saturation time of 5.0 s, 12.0 s relaxation delay, and an
153 acquisition time of 1.7 s for an overall recycle delay of 14 s.[25] Other parameters were 90° pulse
154 of 10.13 μs @ 20 W, spectral width of 19.2 ppm and 32 scans per irradiation frequency (in
155 blocks of 8 scans at each on/off irradiation) and receiver gain of 203.[26]

156 Binding epitopes on each ligand were identified by the presence of ligand signal in the
157 difference spectra. The importance of individual protons in each interaction was evaluated by
158 comparing their relative degrees of saturation. These values were calculated by setting the most
159 intense ligand signal to 100% and normalizing all other signals accordingly, given similar
160 relaxation rates of each hydrogen in the ligand molecules (Figure S3, Table S1).

161

162 **2.3.2 2D NMR**

163 2D NMR samples were prepared with 0.25 mM $\alpha_2$g in 10 mM phosphate buffer, pH 6.8 with
164 15% DMSO-$d_6$. EGCG was added to protein-ligand samples 1 h prior to analysis to achieve a
165 final concentration of 12.5 mM EGCG, or 50-fold ligand excess. All experiments were run at a
166 temperature of 297 K with a spectral width of 20 ppm ($^1$H) and 170 ppm ($^{13}$C). TOCSY
167 experiments were performed using 256 increments and 24 scans for a total time of 63 hours and
168 15 minutes. Mixing times of 20, 45, 65, 75 and 110 ms were used during acquisition of the $\alpha_2$g
169 alone and later merged for assignment of the spectra. A mixing time of 110 ms only was used for
170 acquisition of the $\alpha_2$g/EGCG complex. $^1$H-$^{13}$C HSQC experiments were acquired using 256
171 increments and 136 scans for a total time of 16 hours and 18 minutes.

172 Partial assignment of $\alpha_2$g was achieved based on previously published literature regarding
173 chemical shift values for amino acids leucine, glutamine, proline, phenylalanine and tyrosine.[27,28]

174

175 **2.4 Circular Dichroism**

176 Circular dichroism (CD) spectra were recorded in the far-UV region on a Jasco J-1500 CD
177 spectrometer in a 0.1 mm path length cuvette. Spectra were acquired at every nanometer from
178 160 to 260 nm at 37 °C. EGCG spectra were recorded at each experimental concentration as
179 controls to subtract from the corresponding EGCG/$\alpha_2$g spectra. All spectra were averaged from 3
180 scans. Data were normalized to produce molar residue ellipticity values, smoothed over 5 nm,
181 and plotted with the JASCO spectra manager software. Changes in secondary structure were
182 calculated as changes in relative helicity using the following equation:

183 $$\frac{[\theta]_{222}}{[\theta]_{208}} = \text{relative helicity}$$

184 Effects of concentration and pH were carried out at pH 2.0, 6.8 and 7.5 with concentrations
185 of 0.25 μM $\alpha_2$g and 10-times excess EGCG in 10 mM sodium phosphate buffer using a 1 mm
186 cuvette.
187
188 **2.5 Statistical Analysis**
189 All analyses were repeated in triplicate (n = 3) and analyzed with-one-way ANOVA and two-
190 way ANOVA analysis for samples with varied pH experiments, then paired with Tukey's test for
191 honestly significant differences. Differences of $p < 0.05$ were considered significant. Statistical
192 analysis was performed using GraphPad Prism 6.0 (GraphPad, La Jolla, CA).
193
194 **3 Results and Discussion**
195 **3.1 EGCG interacts with $\alpha_2$g to form insoluble complexes**
196 Upon mixing $\alpha_2$g and EGCG in sodium phosphate buffer (10 mM, pH 6.8), the formation of
197 insoluble aggregates was observed (Figure 1). The physical state of $\alpha_2$g and EGCG appeared to
198 be dependent upon concentration ratio. While colloidal particles were measured at some
199 concentration ratios, a turbidity threshold was reached for others where the upper detection limits
200 of the Viscotek instrument used for DLS were reached, indicating a turbid solution due to haze
201 formation and subsequent phase separation. Colloidal particles were detected at low
202 concentrations protein (0.025 mg/mL) even in the absence of EGCG, and phase separation did
203 not occur even upon the addition of EGCG in 100-times excess of $\alpha_2$g. In contrast, phase
204 separation occurred after the addition of EGCG in only 5-times excess of greater protein
205 concentrations (0.25 mg/mL). This trend is not linear, rather, the turbidity threshold at a given
206 protein concentration appears to decrease in a similar fashion to a one-phase decay. At a

concentration of 0.05 mg/mL $\alpha_2$g, the turbidity threshold was over 75-times excess EGCG, whereas doubling the concentration of protein decreased the relative amount of EGCG required for phase separation by more than half (25-times excess).

### 3.2 Cooperative, non-specific binding interactions drive EGCG-$\alpha_2$gliadin complex formation

Observation of reaction thermodynamics driving the formation of colloidal $\alpha_2$g/EGCG complexes by isothermal titration calorimetry (ITC) demonstrated that $\alpha_2$g contains multiple binding sites for EGCG, resulting in a cooperative, multiphasic reaction (Figure 2). The relatively small exchange of heat observed suggests that these interactions are non-covalent, and the presence of multiple potential binding sites on each reactant suggest that the interaction is multivalent.

While the net energy of the reaction appears to be endothermic, the isotherm generated upon titration of EGCG into $\alpha_2$g demonstrates a complex reaction of both endothermic and exothermic responses upon injection (Figure 2b). Based on the intensity of primary endothermic phase observed suggests initial reactions are driven by hydrophobicity of the peptide and EGCG. Hydrophobic interactions between proline-rich proteins and polyphenols have been well-documented as occurring between ring structures within peptides including aromatic and pyrrolidine rings,[29] both of which are present in $\alpha_2$g in the form of 13 proline residues and 5 aromatic amino acids including phenylalanine and tyrosine. The change in the sign of the complexation enthalpy coincides with a sudden increase in the hydrodynamic radius of the complexes at the onset of the exothermic complexation process. The endothermic response arises from the co-desolvation of the peptide and polyphenol, which displaces water.[30] The weak

230 exothermic reaction is likely derived from the formation of hydrogen bonds, which are able to
231 form between peptide bond carbonyls and phenolic hydroxyl groups.[31] The continuation of
232 endothermic reactions to saturation suggests further hydrophobic interaction which may be due
233 to the aggregation of EGCG/$\alpha_2$g complexes.[20]

234 NMR was used to elucidate binding sites on both EGCG and $\alpha_2$g in STD-NMR and 2D
235 NMR experiments, respectively. These data were used in conjunction with findings from ITC to
236 define the stochiometric characteristics of the interaction based on available interaction sites
237 within the structures of each reactant. STD-NMR is a pseudo-2D experiment in which a receptor
238 (e.g., a protein) is selectively irradiated to transfer saturation signals to areas of the ligand that
239 are in contact with the receptor, resulting in a decreased signal intensity from the free ligand.
240 This also provides information regarding which parts of the ligand are in contact with the
241 receptor.[32] This method allows for semi-quantitative characterization of binding epitopes on
242 ligands through calculation of the relative degree of saturation of each proton involved in the
243 interaction.

244 Interaction between $\alpha_2$-gliadin (57-89) and EGCG was also observed by STD-NMR (Figure
245 3). Localization of more intense STD signals within the structure of EGCG suggest the
246 possibility of preferential binding or interaction specificity (Figure 3c). In a comparison of the
247 overall saturation of each ring constituent of EGCG, the B- and D-rings showed the greatest
248 degree of saturation with no significant difference between one another, regardless of solvent
249 system and visualization of phenolic hydroxyl groups (Figure 3d, Figure S4). All hydrogens on
250 the A- and C-rings show a lesser degree of saturation than those of the B- and D-rings,
251 suggesting further distance from the peptide and a lesser role in the overall interaction. These
252 trends suggest the importance of the EGCG's gallate and galloyl moieties with respect to

253 interaction with $\alpha_2$g. As relative degree of saturation is a measurement of relative spatial
254 proximity between ligand and peptide, one can conclude that the flexibility of the galloyl
255 moieties allow insertion into binding pockets, whereas A- and C-ring hydrogens are more likely
256 to be affected by steric hindrance and play a less meaningful role with respect to their interaction
257 with $\alpha_2$g.

258 2D NMR experiments were performed in order to identify areas within the peptide that are
259 structurally affected upon the formation of EGCG/$\alpha_2$g complexes either as a result of direct
260 binding with EGCG or conformational changes induced by binding elsewhere on the peptide.[33]
261 Crosspeaks were assigned to amino acids based on previously determined chemical shift values
262 and correlation patters with adjustment for solvent effects and neighboring amino acid
263 residues.[21,27]

264 The $^1$H-$^{13}$C HSQC experiment allowed for elucidation of structural changes as observed by
265 changes in $^{13}$C chemical shifts (Figure 4a-c). Superimposition of the EGCG/$\alpha_2$g spectrum over
266 the spectrum of $\alpha_2$g alone shows slight changes in each nucleus, though more pronounced in the
267 proton spectrum as the chemical shift spread is smaller and more sensitive to change. The
268 changes in the HSQC spectra as a result of EGCG addition are primarily 15-30 Hz higher
269 frequency on f2.

270 As $^1$H-$^1$H TOCSY measures correlations between protons in the same spin system, it is
271 helpful for mapping changes within a group of nuclei, such as the R groups of amino acids in a
272 peptide (Figure 4d-g). These data demonstrate primarily high frequency shifts as a result of
273 interaction with EGCG. These shifts can be attributed to binding rather than bulk or solvent
274 effects, as the DMSO-$d_6$ signal remains unchanged between the two spectra. Our findings from
275 ITC demonstrate that the interaction mechanism could not be fit into a one-site binding model,

276 suggesting multiple binding sites. This is corroborated by these findings where changes in
277 chemical shift are not isolated to specific residues. This is unsurprising due to the size and
278 simplicity of the peptide in question, as well as the high frequency of residues that have been
279 implicated as potential binding sites for polyphenolic interaction. Of $\alpha_2$g's primary sequence, 13
280 amino acids are proline and 5 possess aromatic R-groups; thus, 54% of the $\alpha_2$g's amino acids
281 provide potential binding sites for EGCG not including the hydrogen bonding sites.

282 High-frequency shifts observed in the NMR spectra have been shown to result from the
283 binding of aromatic rings between to the peptide of interest, as has been shown previously.[21,33,34]
284 The stacking of aromatic rings between two molecules causes the electron density of that area to
285 increase, inducing the observed high frequency shifts of the proton nuclei, which can be
286 observed most clearly with the tyrosine signals shown in Figure 5b. The greatest shifts noted
287 appeared in the HN-H crosspeak regions shown in Figure 5c, which suggest the importance of
288 the peptide backbone. These shifts may be due to direct interaction and hydrogen bond formation
289 with EGCG or overarching changes to the chemical environment caused by those interactions,
290 such as structural modification.[21]

291 Taken together, the findings from ITC and NMR allow for elucidation of the stoichiometry
292 of the interactions between EGCG and $\alpha_2$g. Based on the inflection point in (I) of the ITC data
293 (Figure 2a), the stoichiometry of the initial endothermic reaction phases can be estimated to be
294 ~5:1 (EGCG:$\alpha_2$g). The formation of insoluble complexes between proline-rich proteins and
295 polyphenols is most favorable at (polyphenol binding site):(protein binding site) ratios of
296 approximately 1:1.[20,35] STD-NMR confirms the presence of 3 identified binding sites per EGCG
297 molecule (phenolic rings A, B, D) and a potential 18 binding sites (proline and aromatic

298 residues) per $\alpha_2$g molecule, the (polyphenol binding site):(protein binding site) ratio can be
299 calculated to be 0.83:1, a favorable condition for complex formation.[20]
300
301 **3.3 Interactions cause subtle changes to protein structure at physiological pH conditions**
302 The physical characteristics of EGCG/$\alpha_2$g complexes were investigated by DLS and CD over
303 the course of titration (Figure 5a). ITC demonstrated that an endothermic reaction occurs as the
304 molar ratio of EGCG:$\alpha_2$g increased from 0-10, at which point the binding isotherm suggests that
305 a point of saturation has been reached.[36] The saturation of binding sites within a peptide by
306 polyphenols has been described previously as the formation of a "polyphenolic coating".[37] Our
307 data show only modest increases in $R_h$ by DLS throughout this titration period. The stacking of
308 phenolic rings onto proline and aromatic residues up to a point of binding site saturation has been
309 documented with other proline-rich proteins with varying implications for particle size that are
310 dependent on both the protein and polyphenol. Where our data show that particle size does not
311 change upon initial interactions with EGCG, other studies have shown decreases in particle size
312 as measured by DLS at this stage. The rationale for the decrease is that complexation with
313 polyphenols may cause proteins to become more compact.[20,38] Though $\alpha_2$g is similar to the
314 salivary proteins used in the majority of these studies in terms of a high frequency of proline
315 residues in tandem repeats within the primary structure, the proline residues in $\alpha_2$g are not
316 mutually adjacent. Moreover, salivary proteins typically feature a high frequency of glycine
317 residues which contribute to the flexibility of the protein backbone; these residues are notably
318 absent from $\alpha_2$g.
319 Increases in $R_h$ of EGCG/$\alpha_2$g complexes were recorded as EGCG concentrations increased
320 beyond 10-times molar excess of $\alpha_2$g. These increases correspond to the weakly exothermic

321 reaction measured by ITC between 10- and 20-times molar excess of EGCG. One explanation
322 for the observed exothermic response is the formation of hydrogen bonds within complexes,
323 which serve to stabilize the complexes. Hydrogen bonds could be occurring between two
324 EGCG/$\alpha_2$g complexes as well via the phenolic hydroxyl groups. The increase in $R_h$ suggests that
325 the latter crosslinking between EGCG/$\alpha_2$g complexes via noncovalent interactions are beginning
326 to occur. As binding site saturation is achieved within the peptide structure, EGCG molecules
327 oriented towards the surface of the complex, or the "polyphenol coating" are able to bind other
328 EGCG or EGCG/$\alpha_2$g complexes, causing the formation of larger intermolecular bridges, or
329 cross-links.[20] This phenomenon explains the sharp increase in $R_h$ measured, which cannot be
330 explained simply by an additive effect of EGCG alone continuing to bind to singular complexes.
331 In the second endothermic phase taking place between 20- and 40-times molar excess of
332 EGCG, continuous growth of particle size is again observed, culminating in a stabilized
333 maximum of 52.9 nm ± 3.5 from 35- to 50-times molar excess EGCG that corresponds to the
334 stabilized $\Delta H_{obs}$ of part IV in Figure 2. The increase in size suggests a large cluster formed by 6
335 to 8 EGCG/$\alpha_2$g complexes. Interestingly, heat is still absorbed by the system even after the $R_h$
336 measurements have reached a plateau. This may be due to additional binding of EGCG to the
337 predominant population of large clusters and a lack of single EGCG/$\alpha_2$g complexes available for
338 further binding to the clusters. It is also possible that two large clusters cannot in turn bind stably
339 with each other due to weak interactions. In addition, the findings from CD experiments suggests
340 that the $\alpha_2$g undergoes structural change, as noted by an increase in $\theta_{222}/\theta_{208}$ as EGCG is titrated
341 into the system beyond 40-times molar excess. An increase in $\theta_{222}/\theta_{208}$ denotes an increase in
342 relative helicity of the $\alpha_2$g, and the heat absorption may be due to the desolvation of functional
343 groups as the peptide undergoes rearrangement within the EGCG/$\alpha_2$g complex system.

344 The ability of EGCG to induce a conformational change in a protein upon binding has been
345 shown previously, notably causing a similar disorder-to-order transition in proline-rich salivary
346 protein IB-5 [21], which shares structural similarities to $\alpha_2$g in terms of molecular weight, primary
347 amino acid sequence and natively unfolded structure. In general, interactions between
348 polyphenols and proline-rich salivary proteins have been shown to be similar to the interactions
349 observed in the present study, in that they are the result of cooperative binding mechanisms and
350 driven by both entropy and enthalpy.[29,30,36,39,40] Polyphenols like EGCG have been shown to
351 interact with multiple areas on a single peptide, causing the peptide to "wrap around" the
352 polyphenols. This results in a modification of the structure of the protein, which was confirmed
353 in the present study by CD.

354 Among the differences in test conditions between these experiments and those previously
355 characterizing proline-rich protein interactions with polyphenols is pH. As a primary interest in
356 these interactions is their contribution to astringency in wine, these systems are often tested at
357 acidic pH (~3.5).[20,21,36,38] Further, variations in concentration have been explored that may affect
358 the course of the reaction. An understanding of the effect that pH plays in terms of protein-
359 phenolic interactions is essential in developing a potential therapy for any disease state involving
360 the digestive tract. Each experiment to this point has been carried out at pH 6.8, characteristic of
361 the duodenojejunal junction, where the symptoms of celiac disease tend to manifest.[15,41]

362 In order to investigate the impact of pH throughout the digestive tract on the complexes
363 formed, DLS and CD were run at pH 2.0. pH 6.8 and pH 7.5. The concentration of $\alpha_2$g was
364 increased tenfold for these experiments. Overall, the trends observed in terms of particle size
365 were not affected by pH, showing that increasing EGCG concentration result in the formation of
366 insoluble complexes (Figure 5b). The notable differences in particle size occur at lower

concentrations ratios. Where increases in $R_h$ were not observed in the initial experiments until after 10-times EGCG concentration was achieved, the increases in particle size observed here are immediate and dependent on pH. At pH 2.0, which represents the gastric environment, larger particles were observed to form upon the first EGCG addition, whereas the increase in particle size is more gradual for higher pH levels. This may be attributed to the stability of EGCG at each pH level as well as the decreased availability of hydrogen bonding partners for EGCG due to protonation of the peptide, resulting in an equilibrium shift towards complexes that feature a greater amount of ring-stacking. Nevertheless, as the titration proceeded in each case, the development of similarly sized particles occurred at the same rate. The plateau of $R_h$ as EGCG:$\alpha_2$g approached 50 suggests that the reaction proceeds in a similar fashion was what was discussed for lower concentrations.

A non-significant change in peptide structure from disordered to ordered was observed at these increased concentrations ($p = 0.08$; Figure 5c); however, the change was observed at only 10-times molar excess of EGCG, which is lower than the observed minimum concentration excess in previous experiments. This is may be due to a phenomenon known as "macromolecular crowding", wherein the reduction in free water caused by increased concentration of macromolecules can induce protein folding and affect conformational stability.[42] The potential for crowding to induce a conformational change in the peptide with lower concentrations of EGCG has important implications for this interaction, as an *in vivo* system would be more complex than what has been tested *in vitro* with these experiments. Though a more complex environment would introduce competition for binding between EGCG and $\alpha_2$g, polyphenols have been shown to bind preferentially to proline-rich proteins and our findings suggest that the

389 presence of potential competitors and other molecules may initiate conformational changes with
390 a lesser amount of available EGCG.
391

392 **4 Conclusions**

393 Our findings demonstrate that interactions between EGCG and $\alpha_2$g occur though four distinct
394 energetic phases which correspond to the formation of insoluble complexes and result in
395 structural modification of the peptide (Figure 6). The initial endothermic phase (I) of the reaction
396 corresponded to hydrophobic interactions as EGCG stacks onto the $\alpha_2$g. Dynamic light scattering
397 revealed increases in $R_h$ of particles through the following weak exothermic phase (II), driven by
398 polar interactions or hydrogen bonding, and further endothermic reactions (III) culminating in
399 the reaction reaching a saturation point (IV). Structural changes to the peptide backbone were
400 characterized by both 2D NMR and CD. Changes in chemical shifts within the HN-Hα
401 crosspeak region of the $^1$H-$^1$H TOCSY spectrum suggested modification to the chemical
402 environment through interactions with or refolding of the peptide backbone. Examination of the
403 relative helicity of the peptide within the EGCG/$\alpha_2$g complex by CD revealed that a structural
404 change did take place, increasing helicity as a result of a disorder-to-order transition.

405 The ability of EGCG to interact with $\alpha_2$g in a range of physiologically relevant environments
406 and to elicit a conformational change on the peptide highlights the potential for polyphenols to
407 be used as a nutraceutical approach to mitigating the symptoms and immune response associated
408 with celiac disease. Previous work has demonstrated that pre-treatment of gliadin proteins with
409 polyphenol-rich green tea extract mitigates gliadin-mediated inflammatory responses and
410 permeability in a cell culture model of celiac disease.[23] Celiac disease pathogenesis is based
411 heavily upon the deamidation of glutamine within gluten peptide fragments and upon the

412 recognition of epitopes containing proline and glutamine residues by immune cells. Each of these
413 potential receptors, TG2 and HLA-DQ2, respectively, feature binding pockets specific to the
414 structural characteristics of gliadin in terms of both amino acid sequence as well as extended
415 structuration.[19,43] Minor changes to amino acids within highly immunogenic gliadin fragments
416 have been shown to greatly decrease recognition by HLA-DQ2 and thus, have the potential to
417 prevent an immune response. Although direct changes to the amino acid sequence (i.e.
418 substitution) *in vivo* would be impossible, these findings support the potential for development of
419 a post-digestion mechanism for blocking gliadin peptide recognition through sequestration of
420 binding epitopes and structural modification of the immunostimulatory peptide.
421 Interactions between gliadin proteins and dietary polyphenols from green tea have been
422 studied in other *in vitro* systems which highlight other factors beyond pH which may affect the
423 formation and stability of the complexes observed in this study. These studies demonstrated the
424 propensity of tea polyphenols to interact with both native and hydrolyzed gliadins, as well as the
425 protective effects of polyphenols against gliadin-mediated inflammation and permeability in a
426 cell culture model of the small intestine.[23] At this time, the protective effects of polyphenols
427 against gliadin has not been tested *in vivo*, though gliadin sequestration via synthetic polymer
428 systems that interact with the protein in a similar manner have been shown to prevent celiac-
429 associated immune responses in gliadin sensitized mice.[44,45] The comprehensive approach taken
430 in this study to examine physical and chemical interactions between $\alpha_2$g and EGCG in
431 physiologically relevant environments provides the foundation for further exploration of EGCG
432 and other dietary polyphenol as therapeutic or protective agents within the context of celiac
433 disease.
434

435 **Conflict of Interest**

436 The authors declare no competing financial interest.

437

438 **Acknowledgements**

439 The authors would like to thank Julia A. Fecko from the Penn State Automated Biological
440 Calorimetry Facility for her help with training on instrumentation and assistance in optimizing
441 ITC experiments. This project was supported by a National Institute of Food and Agriculture
442 Predoctoral Fellowship awarded to C. V. under Grant no. 2016-67011-24702, USDA Agriculture
443 and Food Research Initiative. ITC, DLS and CD experiments were performed at the Penn State
444 Automated Biological Calorimetry Facility – University Park, PA thanks in part to the NSF-MRI
445 award DBI-0922974.

446

447 **References**

448 1. K. Kim, T. M. Vance, O. K. Chun, Estimated intake and major food sources of flavonoids among
449 US adults: changes between 1999–2002 and 2007–2010 in NHANES. *Eur. J. Nutr.*, 2016, **55**,
450 833–843.

451 2. J. D. Lambert, C. S. Yang, Cancer chemopreventive activity and bioavailability of tea and tea
452 polyphenols. *Mutat. Res. - Fundam. Mol. Mech. Mutagen.*, 2003, **523–524**, 201–208.

453 3. M. Bose *et al.*, The major green tea polyphenol, (-)-epigallocatechin-3-gallate, inhibits obesity,
454 metabolic syndrome, and fatty liver disease in high-fat-fed mice. *J. Nutr.*, 2008, **138**, 1677–83.

455 4. C. S. Yang, J. M. Landau, Effects of tea consumption on nutrition and health. *J. Nutr.*, 2000, **130**,
456 2409–2412.

457 5. J. V Higdon, B. Frei, Tea catechins and polyphenols: health effects, metabolism, and antioxidant
458 functions. *Crit. Rev. Food Sci. Nutr.*, 2003, **43**, 89–143.
459 6. M. Brückner, S. Westphal, W. Domschke, T. Kucharzik, A. Lügering, Green tea polyphenol
460 epigallocatechin-3-gallate shows therapeutic antioxidative effects in a murine model of colitis. *J.*
461 *Crohn's Colitis*., 2012, **6**, 226–235.
462 7. J. Vesić, I. Stambolić, D. Apostolović, M. Milčić, D. Stanic-Vucinic, T. C. Velickovic,
463 Complexes of green tea polyphenol, epigalocatechin-3-gallate, and 2S albumins of peanut. *Food*
464 *Chem.*, 2015, **185**, 309–317.
465 8. J. Ognjenović, M. Stojadinović, M. Milčić, D. Apostolović, J. Vesić, I. Stambolić, M.
466 Atanasković-Marković, M. Simonović, T. C. Velickovic, Interactions of epigallo-catechin 3-
467 gallate and ovalbumin, the major allergen of egg white. *Food Chem.*, 2014, **164**, 36–43.
468 9. H. S. Oz, T. Chen, W. J. S. De Villiers, Green tea polyphenols and sulfasalazine have parallel
469 anti-inflammatory properties in colitis models. *Front. Immunol.*, 2013, **4**, 1–10.
470 10. N. J. Plundrich, M. Kulis, B. L. White, M. H. Grace, R. Guo, A. W. Burks, J. P. Davis, M. A.
471 Lila, Novel strategy to create hypoallergenic peanut protein-polyphenol edible matrices for oral
472 immunotherapy. *J. Agric. Food Chem.*, 2014, **62**, 7010–21.
473 11. F. Yang, W. J. S. De Villiers, C. J. McClain, G. W. Varilek, Green Tea Polyphenols Block
474 Endotoxin-Induced Tumor Necrosis Factor- Production and Lethality in a Murine Model. *J. Nutr.*,
475 1998, **128**, 2334–2340.
476 12. E. Melgarejo, M. Á. Medina, F. Sánchez-Jiménez, L. M. Botana, M. Domínguez, L. Escribano,
477 A. Orfao, J. L. Urdiales. (-)-Epigallocatechin-3-gallate interferes with mast cell adhesiveness,
478 migration and its potential to recruit monocytes. *Cell. Mol. Life Sci.*, 2007, **64**, 2690–2701.

479 13. E. Melgarejo, M. Á. Medina, Targeting of histamine producing cells by EGCG: a green dart
480 against inflammation? *J Physiol Biochem.*, 2010, **66**, 3, 265–270.
481 14. N. J. Plundrich, R. R. Bansode, E. A. Foegeding, L. L. Williams, M. A. Lila, Protein-bound
482 Vaccinium fruit polyphenols decrease IgE binding to peanut allergens and RBL-2H3 mast cell
483 degranulation in vitro. *Food Funct.*, 2017, **8**, 1611–1621.
484 15. A. Fasano, C. Catassi, Celiac Disease. *New Engl. J. Med.*, 2007, **367**, 1731–1743.
485 16. M. Kreis, B. G. Forde, S. Rahman, B. J. Miflin, P. R. Shewry, Molecular evolution of the seed
486 storage proteins of barley, rye and wheat. *J. Mol. Biol.*, 1985, **183**, 499–502.
487 17. L. W. Vader, A. de Ru, Y. van der Wal, Y. M. C. Kooy, W. Benckhuijsen, M. L. Mearin, J. W.
488 Drijfhout, P. van Veelen, F. Koning, Specificity of tissue transglutaminase explains cereal
489 toxicity in celiac disease. *J. Exp. Med.*, 2002, **195**, 643–9.
490 18. C. Catassi, E. Fabiani, G. Iacono, C. D'Agate, R. Francavilla, F. Biagi, U. Volta, S. Accomando,
491 A. Picarelli, I. De Vitis, G. Pianelli, R. Gesuita, F. Carle, A. Mandolesi, I. Bearzi, A. Fasano, A
492 prospective, double-blind, placebo-controlled trial to establish a safe gluten threshold for patients
493 with celiac disease. *Am. J. Clin. Nutr.*, 2007, **85**, 160–6.
494 19. C.-Y. Kim, H. Quarsten, E. Bergseng, C. Khosla, L. M. Sollid, Structural basis for HLA-DQ2-
495 mediated presentation of gluten epitopes in celiac disease. *Proc. Natl. Acad. Sci. U. S. A.*, 2004,
496 **101**, 4175–9.
497 20. E. Jöbstl, J. O'Connell, J. P. Fairclough, M. P. Williamson, Molecular model for astringency
498 produced by polyphenol/protein interactions. *Biomacromolecules.*, 2004, **5**, 942–9.
499 21. C. Pascal, F. Paté, V. Cheynier, M. A. Delsuc, Study of the interactions between a proline-rich
500 protein and a flavan-3-ol by NMR: Residual structures in the natively unfolded protein provides
501 anchorage points for the ligands. *Biopolymers.*, 2009, **91**, 745–756.

502 22. M. G. Herrera, F. Zamarreño, M. Costabel, H. Ritacco, A. Hütten, N. Sewald, V. I. Dodero,
503 Circular dichroism and electron microscopy studies in vitro of 33-mer gliadin peptide revealed
504 secondary structure transition and supramolecular organization. *Biopolymers*., 2014, **101**, 96–106.
505 23. C. B. Van Buiten, J. D. Lambert, R. J. Elias, Green Tea Polyphenols Mitigate Gliadin-Mediated
506 Inflammation and Permeability in Vitro. *Mol. Nutr. Food Res.*, 2018, **1700879**, 1–8.
507 24. K. Stott, J. Stonehouse, J. Keeler, T.-L. Hwang, A. J. Shaka, Excitation Sculpting in High-
508 Resolution Nuclear Magnetic Resonance Spectroscopy: Application to Selective NOE
509 Experiments. *J. Am. Chem. Soc.*, 1995, **117**, 4199–4200.
510 25. H. Green, S. Wimperis, R. Freeman, Band-Selective Pulses without Phase Distortion. A
511 Simulated Annealing Approach. *J. Magn. Reson.*, 1989, **85**, 620–627.
512 26. A. Viegas, J. Manso, F. L. Nobrega, E. J. Cabrita, Saturation-Transfer Difference (STD) NMR: A
513 Simple and Fast Method for Ligand Screening and Characterization of Protein Binding. *J. Chem.*
514 *Educ.*, 2011, **88**, 990–994.
515 27. D. S. Wishart, C. G. Bigam, A. Holm, R. S. Hodges, B. D. Sykes, 1H, 13C and 15N random coil
516 NMR chemical shifts of the common amino acids. I. Investigations of nearest-neighbor effects. *J.*
517 *Biomol. NMR*., 1995, **5**, 67–81.
518 28. S. Schwarzinger, G. J. A. Kroos, T. R. Foss, J. Chung, P. E. Wright, H. J. Dyson, Sequence-
519 dependent correction of random coil NMR chemical shifts. *J. Am. Chem. Soc.*, 2001, **123**, 2970–
520 2978.
521 29. A. J. Charlton, N. J. Baxter, M. L. Kahn, A. J. G. Moir, E. Haslam, A. P. Davies, M. P.
522 Williamson, Polyphenol/peptide binding and precipitation. *J. Agric. Food Chem.*, 2001, **50**,
523 1593–601.

524 30. O. Callies, A. Hernández Daranas, Application of isothermal titration calorimetry as a tool to
525 study natural product interactions. *Nat. Prod. Rep.*, 2016, **33**, 881–904.
526 31. K. J. Siebert, A. Carrasco, P. Y. Lynn, Formation of Protein−Polyphenol Haze in Beverages. *J.*
527 *Agric. Food Chem.*, 1996, **44**, 1997–2005.
528 32. M. Mayer, B. Meyer, Group epitope mapping by saturation transfer difference NMR to identify
529 segments of a ligand in direct contact with a protein receptor. *J. Am. Chem. Soc.*, 2001, **123**,
530 6108–6117.
531 33. N. J. Murray, M. P. Williamson, T. H. Lilley, E. Haslam, Study of the interaction between
532 salivary proline-rich proteins and a polyphenol by 1H-NMR spectroscopy. *Eur J Biochem*., 1994,
533 **219**, 923–935.
534 34. N. J. Baxter, T. H. Lilley, E. Haslam, M. P. Williamson, Multiple Interactions between
535 Polyphenols and a Salivary Proline-Rich Protein Repeat Result in Complexation and
536 Precipitation. *Biochem.*, 1997, **36**, 18, 5566–5577.
537 35. K. J. Siebert, N. V. Troukhanova, P. Y. Lynn, Nature of Polyphenol−Protein Interactions. *J.*
538 *Agric. Food Chem.*, 1996, **44**, 80–85.
539 36. C. Pascal, C. Poncet-Legrand, A. Imberty, C. Gautier, P. Sarni-Manchado, V. Cheynier, A.
540 Vernhet, Interactions between a non glycosylated human proline-rich protein and flavan-3-ols are
541 affected by protein concentration and polyphenol/protein ratio. *J. Agric. Food Chem.*, 2007, **55**,
542 4895–901.
543 37. N. Bordenave, B. R. Hamaker, M. G. Ferruzzi, Nature and consequences of non-covalent
544 interactions between flavonoids and macronutrients in foods. *Food Funct.*, 2014, **5**, 18–34.

545 38. C. Poncet-Legrand, A. Edelmann, J. Putaux, D. Cartalade, P. Sarni-Manchado, A. Vernhet,
546 Poly(l-proline) interactions with flavan-3-ols units: Influence of the molecular structure and the
547 polyphenol/protein ratio. *Food Hydrocoll.*, 2006, **20**, 687–697.
548 39. A. J. Charlton, N. J. Baxter, T. H. Lilley, E. Haslam, C. J. McDonald, M. P. Williamson, Tannin
549 interactions with a full-length human salivary proline-rich protein display a stronger affinity than
550 with single proline-rich repeats. *FEBS Lett.*, 1996, **382**, 289–92.
551 40. C. Le Bourvellec, C. M. G. C. Renard, Interactions between Polyphenols and Macromolecules:
552 Quantification Methods and Mechanisms. *Crit. Rev. Food Sci. Nutr.*, 2012, **52**, 3, 213–248.
553 41. D. F. Evans, G. Pye, R. Bramley, A. G. Clark, T. J. Dyson, J. D. Hardcastle, Measurement of
554 gastrointestinal pH profiles in normal ambulant human subjects. *Gut*., 1988, **29**, 1035–41.
555 42. I. M. Kuznetsova, K. K. Turoverov, V. N. Uversky, What Macromolecular Crowding Can Do to a
556 Protein. *Int. J. Mol. Sci.*, 2014, **15**, 23090–23140.
557 43. J. L. Piper, G. M. Gray, C. Khosla, High selectivity of human tissue transglutaminase for
558 immunoactive gliadin peptides: Implications for Celiac Sprue. *Biochemistry*., 2002, **41**, 386–393.
559 44. M. Pinier, G. Fuhrmann, H. J. Galipeau, N. Rivard, J. A. Murray, C. S. David, H. Drasarova, K.
560 Tuckova, J.-C. Leroux, E. F. Verdu. The copolymer P(HEMA-co-SS) binds gluten and reduces
561 immune response in gluten-sensitized mice and human tissues. *Gastroenterology*., 2012, **142**,
562 316–325.
563 45. M. Pinier, E. F. Verdu, M. Nasser-Eddine, C. S. David, A. Vézina, N. Rivard, J.-C.
564 Leroux, Polymeric binders suppress gliadin-induced toxicity in the intestinal epithelium.
565 *Gastroenterology*., 2009, **136**, 288–98.
566

567 **Figure Captions**

568 **Figure 1** Formation of insoluble $\alpha_2$g/EGCG complexes at pH 6.8 as a function of protein
569 content. Markers indicate $\alpha_2$g/EGCG combinations that were measured by DLS for the presence
570 of colloidal aggregates (□) or turbidity (■). The dotted line indicates the one-phase decay of
571 EGCG excess required for phase separation as a function of protein concentration.
572
573 **Figure 2** Titration of EGCG into $\alpha_2$g results in a multiphasic interaction as measured by
574 ITC. (a) Raw ITC data of EGCG titration (3.2 mM) into $\alpha_2$g (12.8 mM). Sections I-IV
575 correspond to areas of structural changes as defined by DLS and CD. (b) The raw data
576 demonstrated a complex isotherm of both endothermic and exothermic reactions upon injection.
577 (c) EGCG titration into buffer yielded weak endothermic responses, which were subtracted from
578 the data.
579
580 **Figure 3** EGCG/$\alpha_2$g interactions are localized to galloyl moieties on EGCG. The following
581 descriptions corresponds to spectra a-c, which were recorded in 85% $H_2O$, 15% DMSO-$d_6$: (a)
582 $^1$H NMR spectrum of EGCG (25 mM) and (b) the corresponding difference spectrum. (c)
583 Relative degree of saturation of EGCG hydrogens upon interaction with $\alpha_2$-gliadin (57-89)
584 normalized to that of H-9,13. (d) Average relative degrees of saturation per EGCG ring
585 constituent. Different letters denote significant differences in relative degree of saturation
586 between ring constituents ($p \leq 0.05$).
587
588 **Figure 4** Superimposition of 2D NMR spectra of $\alpha_2$g before (gray) and after (multicolor)
589 addition of EGCG recorded in 10 mM sodium phosphate buffer, pH 6.8 with 15% v/v DMSO-$d_6$.
590 (a) Full $^1$H-$^{13}$C HSQC spectrum; (b) comparison of aromatic crosspeak region demonstrates

591 shifts in phenylalanine and tyrosine; (c) comparison of the aliphatic sidechain crosspeak region
592 demonstrates shifts in proline, leucine and glutamine. (d) Full $^{1}H$-$^{1}H$ TOCSY spectrum; (e)
593 comparison of the aromatic crosspeak region demonstrating shifting of tyrosine crosspeaks; (f)
594 comparison of sidechain HN and HN-Hα crosspeak regions demonstrating changes in glutamine,
595 leucine and phenylalanine chemical shifts; (g) comparison of Hα/Hβ crosspeak regions
596 demonstrating changes in chemical shift of glutamine and proline.
597
598 **Figure 5** Relationship between particle size and peptide structure to concentration ratios of
599 EGCG to $\alpha_2$g. (a) Hydrodynamic radii of EGCG/$\alpha_2$g complexes (■, solid line) increase as a
600 function of EGCG:$\alpha_2$g. This increase in particle size precedes an increase in peptide helicity (□,
601 dotted line) as measured by $\theta_{222}/\theta_{208}$, which is also dependent on EGCG:$\alpha_2$g. (b) EGCG/$\alpha_2$g
602 aggregate particle sizes (a) increase as a function of EGCG concentration at pH 2.0, 6.8 and 7.5.
603 Particle size is affected by both EGCG concentration and pH ($p < 0.001$) and the interaction
604 between the two parameters ($p = 0.004$). (c) Circular dichroism of $\alpha_2$g upon addition of excess
605 EGCG. Changes in relative helicity of α2g in the presence of 250 μM EGCG (EGCG:α2g = 10).
606
607 **Figure 6** Schematic representation of observed interaction and physical implications of
608 EGCG/$\alpha_2$g complex formation based on ITC, DLS, NMR and CD. Initial samples of $\alpha_2$g exhibit
609 $R_h$ (represented by dotted lines) that do not change significantly over the course of the
610 endothermic reactions taking place during phase I of the titration. As EGCG stacks onto $\alpha_2$g,
611 evidence of weak exothermic reactions suggests the formation of hydrogen bonds and
612 crosslinking between protein-polyphenol complexes, supported by increasing $R_h$. Further

613 endothermic reactions coincide with continued increasing $R_h$ up to a point where particle size no

614 longer increases, but NMR and CD suggest structural change to the peptide backbone.

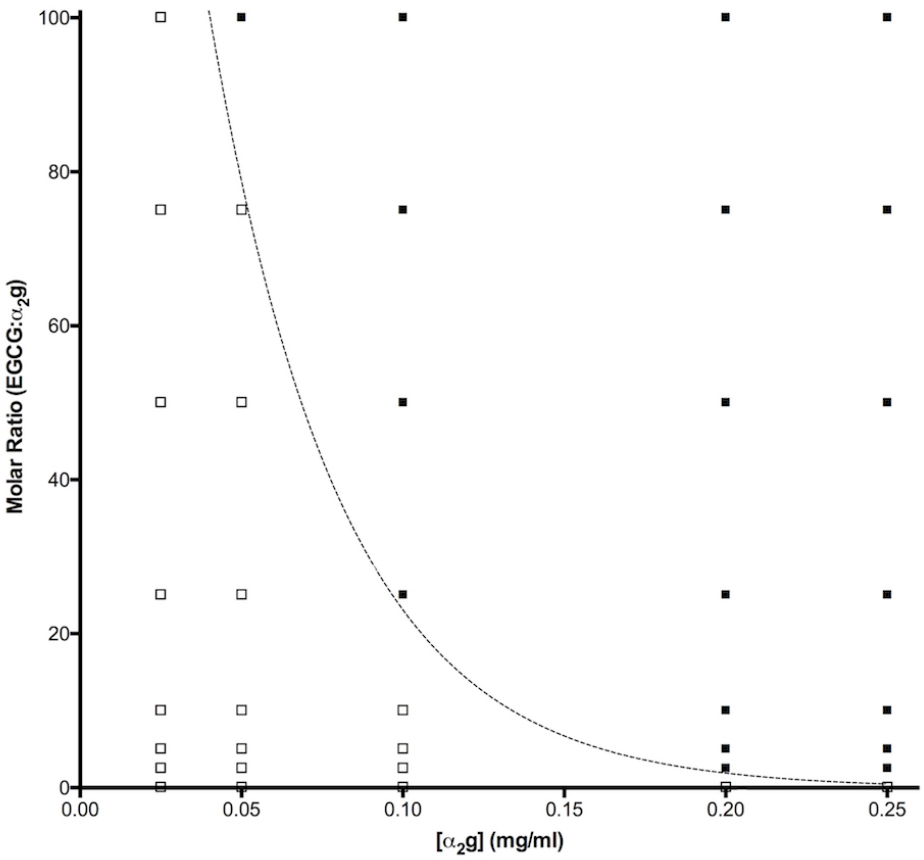


Figure 1. Formation of insoluble α2g/EGCG complexes at pH 6.8 as a function of protein content. Markers indicate α2g/EGCG combinations that were measured by DLS for the presence of colloidal aggregates (□) or turbidity (□). The dotted line indicates the one-phase decay of EGCG excess required for phase separation as a function of protein concentration.

82x75mm (300 x 300 DPI)

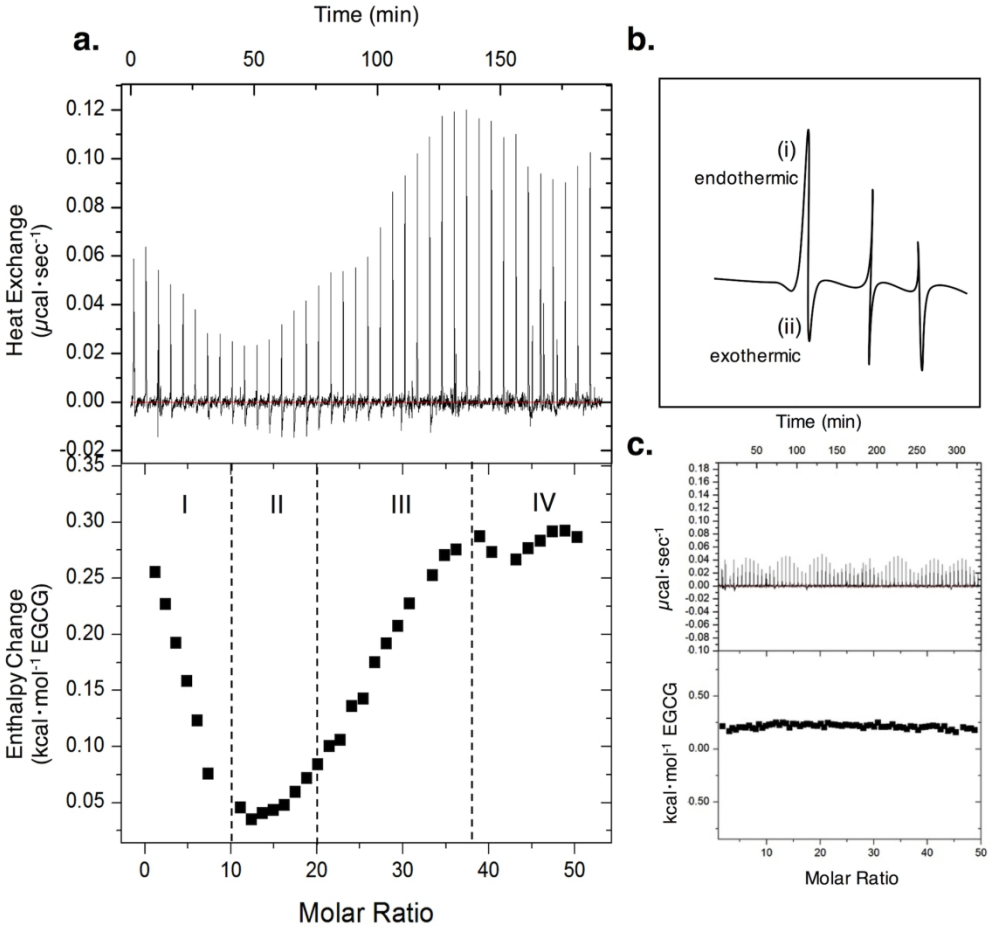


Figure 2 Titration of EGCG into α2g results in a multiphasic interaction as measured by ITC. (a) Raw ITC data of EGCG titration (3.2 mM) into α2g (12.8 mM). Sections I-IV correspond to areas of structural changes as defined by DLS and CiDi. (b) The raw data demonstrated a complex isotherm of both endothermic and exothermic reactions upon injection. (c) EGCG titration into buffer yielded weak endothermic responses, which were subtracted from the data.

171x165mm (300 x 300 DPI)

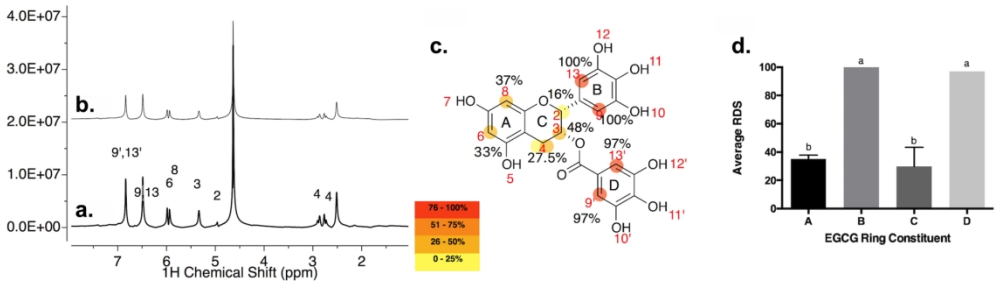


Figure 3 EGCG/α2g interactions are localized to galloyl moieties on EGCG. The following descriptions corresponds to spectra a-c, which were recorded in 85% H2O, 15% DMSO-d6: (a) 1H NMR spectrum of EGCG (25 mM) and (b) the corresponding difference spectrum. (c) Relative degree of saturation of EGCG hydrogens upon interaction with α2-gliadin (57-89) normalized to that of H-9,13. (d) Average relative degrees of saturation per EGCG ring constituent. Different letters denote significant differences in relative degree of saturation between ring constituents ($p \leq 0.05$).

171x50mm (300 x 300 DPI)

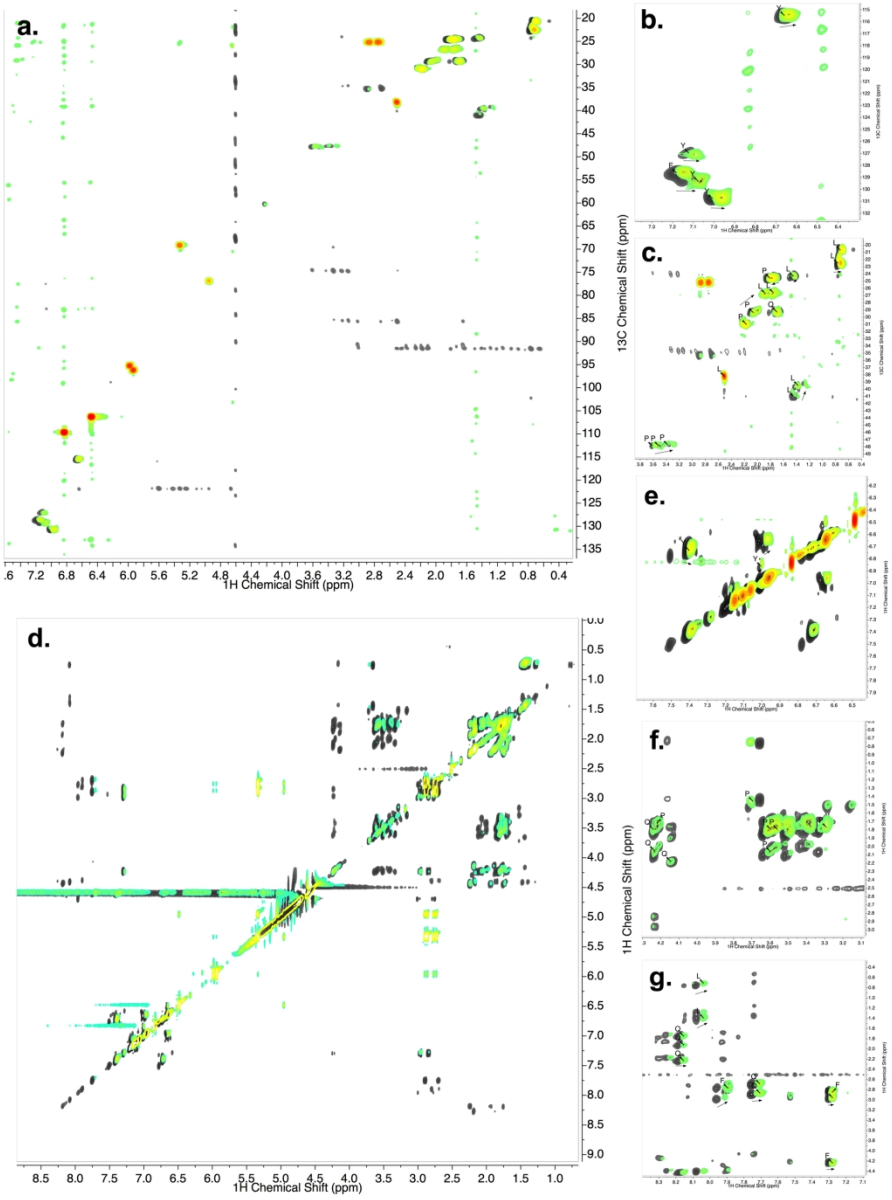


Figure 4 Superimposition of 2D NMR spectra of α2g before (gray) and after (multicolor) addition of EGCG recorded in 10 mM sodium phosphate buffer, pH 6.8 with 15% v/v DMSO-d6. (a) Full 1H-13C HSQC spectrum; (b) comparison of aromatic crosspeak region demonstrates shifts in phenylalanine and tyrosine; (c) comparison of the aliphatic sidechain crosspeak region demonstrates shifts in proline, leucine and glutamine. (d) Full 1H-1H TOCSY spectrum; (e)comparison of the aromatic crosspeak region demonstrating shifting of tyrosine crosspeaks; (f) comparison of sidechain HN and HN-Hα crosspeak regions demonstrating changes in glutamine, leucine and phenylalanine chemical shifts; (g) comparison of Hα/Hβ crosspeak regions demonstrating changes in chemical shift of glutamine and proline.

171x230mm (300 x 300 DPI)

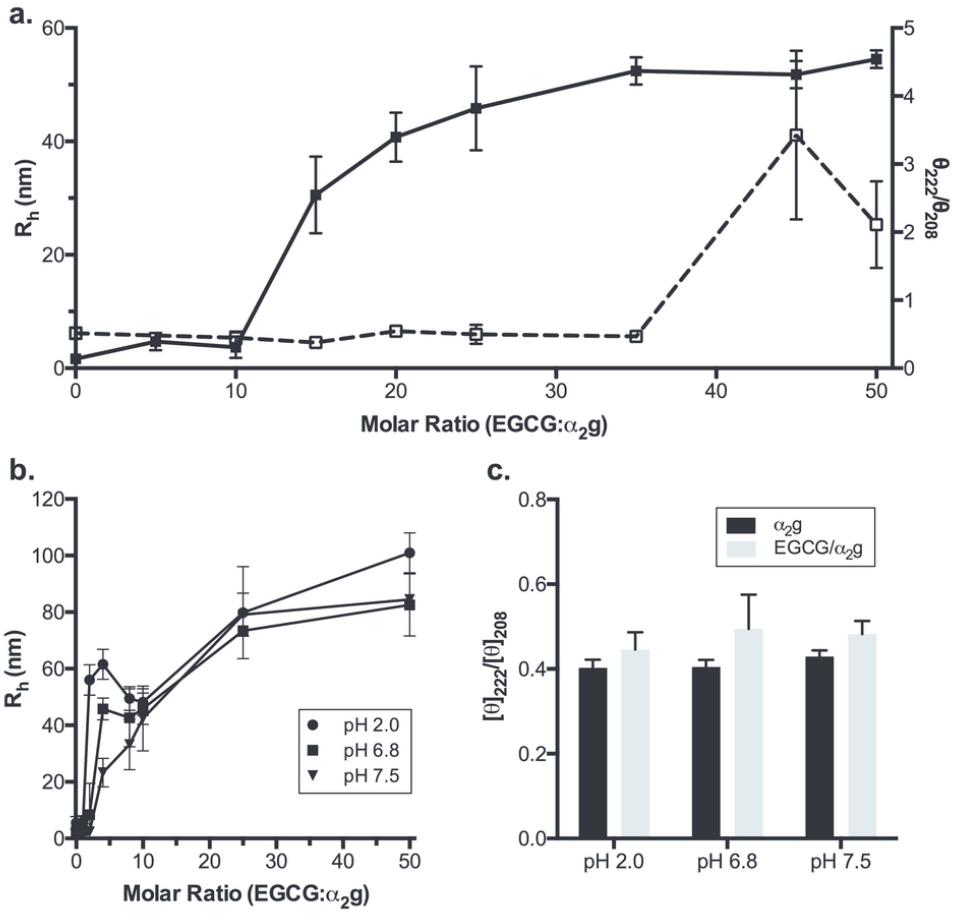


Figure 5. Relationship between particle size and peptide structure to concentration ratios of EGCG to α2g. (a) Hydrodynamic radii of EGCG/α2g complexes (□, solid line) increase as a function of EGCG:α2g. This increase in particle size precedes an increase in peptide helicity (□, dotted line) as measured by $\theta_{222}/\theta_{208}$, which is also dependent on EGCG:α2g. (b) EGCG/α2g aggregate particle sizes (a) increase as a function of EGCG concentration at pH 2.0, 6.8 and 7.5. Particle size is affected by both EGCG concentration and pH ($p < 0.001$) and the interaction between the two parameters ($p = 0.004$). (c) Circular dichroism of α2g upon addition of excess EGCG. Changes in relative helicity of α2g in the presence of 250 μM EGCG (EGCG:α2g = 10).

83x78mm (300 x 300 DPI)

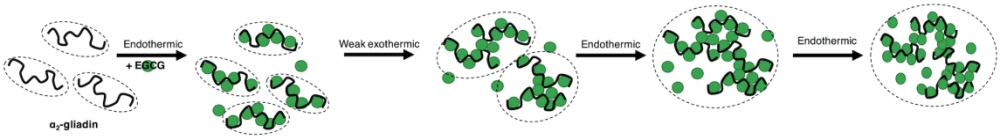


Figure 6 Schematic representation of observed interaction and physical implications of EGCG/α2g complex formation based on ITC, DLS, NMR and CiDi. Initial samples of α2g exhibit $R_h$ (represented by dotted lines) that do not change significantly over the course of the endothermic reactions taking place during phase I of the titration. As EGCG stacks onto α2g, evidence of weak exothermic reactions suggests the formation of hydrogen bonds and crosslinking between protein-polyphenol complexes, supported by increasing $R_h$. Further endothermic reactions coincide with continued increasing $R_h$ up to a point where particle size no longer increases, but NMR and CiDi suggest structural change to the peptide backbone.

171x23mm (300 x 300 DPI)

(-)-Epigallocatechin-3-gallate interacts with celiac-relevant peptide α2-gliadin (57-89) in a multi-phase reaction to form protein-polyphenol complexes in physiologically relevant conditions.

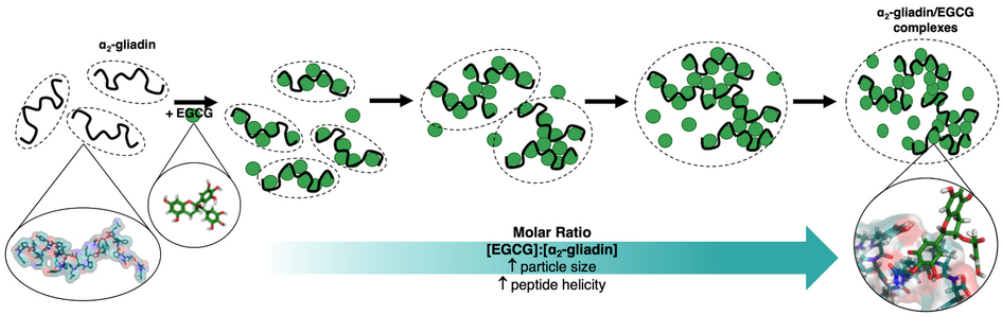


79x25mm (300 x 300 DPI)